pH Responsive Heteroarm Starlike Micelles from Double Hydrophilic ABC Terpolymer with Ampholitic A and C Blocks

Vasiliki Sfika and Constantinos Tsitsilianis*

Department of Chemical Engineering, University of Patras, 26504 Patras, Greece, and Institute of Chemical Engineering and High-Temperature Chemical Processes, ICE/HT-FORTH, P.O. Box 1414, 26504 Patras, Greece

Anton Kiriy,* Ganna Gorodyska, and Manfred Stamm

Institut für Polymerforschung Dresden, Hohe Strasse 6, 01069 Dresden, Germany

Received July 8, 2004; Revised Manuscript Received September 22, 2004

ABSTRACT: We report on the phase behavior and micellization phenomena of a poly(2-vinylpyridine-*b*-poly(methyl methacrylate)-*b*-(poly(acrylic acid) block terpolymer (P2VP−PMMA−PAA) in aqueous dilute solutions. This double hydrophilic terpolymer exhibits different self-assemblies depending on the pH of the solution. At low pH (1−2) heteroarm starlike micelles are formed bearing interactive P2VP and PAA arms in the corona. Aging phenomena due to intramicelleral interactions lead to morphology changes from Janus (segregated arms) to shell cross-linked micelles (mixed arms). As the pH increases from 2 to 3, electrostatic intermicellar attractive interactions rise leading to the formation of nonregular aggregates. An insoluble two-phase region around the isoelectric point of the ampholitic chains was observed between pH 3.2 and 5.8. Finally, at higher pH, an unexpected probably out-of-equilibrium morphology of aggregated amphiphilic heteroarm starlike micelles was observed after deposition on the mica substrate.

Introduction

Over the last few years, much interest has been devoted to the study of block polyampholytes, also named zwitterionic block copolymers, which contain in the same macromolecule weak anionic and cationic polyelectrolyte blocks. The pH dependence of the ionization ability of these blocks has fundamental consequences on the behavior of the copolymer in aqueous media. In a certain pH range these copolymers may exist in molecular dissolution state while they self-assemble in other pH regions. Such stimuli responsive polymeric systems attract the interest of several research groups because of their interesting potential applications for instance in drug delivery systems and water-born formulations.[1]

Recently we demonstrated for the first time how a water-soluble asymmetric triblock copolymer i.e., poly(acrylic acid)-*b*-poly(vinylpyridine)-*b*-poly(acrylic acid) (PAA_{134}−$P2VP_{628}$−PAA_{134}) can be self-organized reversibly into two distinct and completely different structures (i.e., from a transient three-dimensional network to compact micelles) by switching the pH of the aqueous media.[2] More precisely three distinct pH regions were observed. In the high pH region compact micelles with P2VP hydrophobic cores and PAA positively charged chains in the corona were formed. In the intermediate pH region and around the isoelectric point the polymer precipitates. Finally in the low pH region and at low concentrations the polymer is molecularly dissolved. A novel behavior was observed at pH 3.4 (close to the phase separation limit) and at relatively elevated concentrations. Despite the lack of hydrophobic blocks (which play the role of stickers in physical gelation phenomena) this polymer self-assembles to a three-dimensional transient network through electrostatic interactions. The so-formed physical gel exhibits unique rheological properties.[3]

ABC triblock terpolymers comprise a relatively new and interesting research area, as these novel block copolymers consist of three chemically different components, each one conferring to the polymer one different function. Attention was received first on the synthesis and the properties of ABC copolymers in the bulk state. Provided that sufficient incompatibility exists between the blocks, this type of copolymers can form three phases in the bulk,[4] leading to novel morphologies which depend on the volume fractions and the interaction parameters of the copolymer components.[5−9]

In the recent years an increasing number of work have appeared concerning the behavior of the ABC terpolymers in solution.[10−19] ABC triblock polyampholytes have been synthesized by group transfer polymerization (GTP) and their behavior was explored in aqueous solutions. As reported, the size of the micelles strongly depended on the block sequence.[13,15] Moreover these triblocks with the ampholytic character (acidic and basic blocks) show a strong tendency to precipitate near the isoelectric point. Analogous behavior was observed with ABC polyampholytes synthesized by sequential living anionic polymerization.[16]

Micelles of spherical shape were prepared in water by ABC (A, B hydrophobic; C hydrophilic) triblock copolymers. A core−shell structure was obtained the core of which is constituted of two concentric layers.[17] Eisenberg et al. have investigated crew cut aggregates formed from ABC triblock copolymers.[18,19] A number of morphologies such as spherical, rodlike, and vesicular aggregates were observed depending on the solvent chosen and conditions used.

ABC block terpolymers have also been used to produce cross-linked micellar nanostructures. Stimuli responsive "onion" type micelles formed by hydrophilic PEO−PDMEMA−PDEEMA terpolymers were shell

* Corresponding authors. E-mail: (C.T.) ct@chemeng.upatras.gr; (A.K.) kiriy@ipfdd.de.

10.1021/ma048621q CCC: $27.50
Published on Web 11/16/2004

cross-linked by selective quaternization reaction of the poly(2-(diethylamino)ethyl methacrylate) (PDEEMA). These micellar nanoparticles exhibit reversible swelling on varying the solution pH.[20] By cross-linking the middle block of an ABC linear copolymer from its phase separated solid state, heteroarm star copolymers with presegregated different arms can be prepared, which are also named Janus micelles.[21,22]

The association behavior of polystyrene−poly(2-vinylpyridine)−poly(methyl methacrylate) (PS−P2VP−PMMA) ABC triblock copolymers in toluene, which is a nonsolvent for the middle (B) block and common good solvent for the outer A and C blocks, have been studied recently.[23] The micelles formed by such copolymers exhibit a core−shell structure constituted from a B core bearing the A and C block-chains in the corona. These type of micelles were referred to as "heteroarm star"-like micelles since their structures are similar to those of the heteroarm star copolymers prepared by "living" polymerization techniques.[24]

In the present work we have designed and studied a water-soluble amphoteric ABC terpolymer which has the ability to form "heteroarm star"-like micelles due to the hydrophobic nature of the middle block. More precisely, a model poly(2-vinylpyridine)-*b*-poly(methyl methacrylate)-*b*-poly(acrylic acid) (P2VP−PMMA−PAA) block terpolymer was synthesized by anionic polymerization, and explored in aqueous media. The coexistence of a hydrophobic middle block (PMMA) with nearly symmetric anionic (PAA) and cationic (P2VP) weak polyelectrolytes as outer blocks, results in a stimulus responsive ABC terpolymer, which exhibits rich association behavior in water.

Experimental Part

Materials. Tetrahydrofuran (THF) was purified from protonic impurities according to standard procedures. Styrene was distilled twice from sodium wire under vacuum. *sec*-Butyllithium (^{s}BuLi) was prepared from 2-chlorobutane and Li metal in benzene. 2-Vinylpyridine (2VP) was distilled twice, on sodium wire and then on calcium hydride. Methyl methacrylate (MMA) and *tert*-butyl acrylate (tBA) (Merck) were first vacuum distilled on calcium hydride and then treated with triethylaluminum (10% solution in heptane). Once the monomer turned slightly yellow, it was immediately vacuum distilled into a buret.

Polymer Synthesis and Characterization. A two-step procedure was followed to obtain the final P2VP−PMMA−PAA copolymer: First a P2VP−PMMA−PtBA polymer precursor was synthesized by anionic polymerization, then acid hydrolysis gave the desired P2VP−PMMA−PAA. Vinyl-2 pyridine was first polymerized, in THF at −75 °C, using *sec*-butyllithium as initiator in the presence of a 5-fold excess of LiCl. Then at −65 °C the second monomer methyl methacrylate and next *tert*-butyl acrylate were added dropwise. The sudden color change confirmed the rapid and quantitative initiation of the second monomer polymerization. For every step, sampling out from the reaction media was performed, for further characterization. The polymerization was terminated by the addition of a small amount of methanol.

The P2VP−PMMA−PtBA polymer precursor was subjected to acid hydrolysis with a 5-fold excess of concentrated HCl, at 80 °C by reflux in 1,4 dioxane during 12 h. The hydrolysis degree of the copolymer was determined by ^{1}H NMR in deuterated MeOH:$CDCl_3$ (3:1) and also by potentiometric titration using 0.1 N NaOH. The resulting P2VP−PMMA−PAA was diluted in water and purified by dialysis.

The P2VP−PMMA−PtBA precursor was characterized by SEC, static light scattering, and ^{1}H NMR, and its molecular characteristics are shown in Table 1, where the numbers of repeating units for each block are noted as indices. Provided that almost quantitative selective hydrolysis of the PtBA block was achieved the number of the repeating units in the P2VP−PMMA−PAA remains the same with those of its precursor. Hereafter the final product will be designated as $P2VP_{260}$−$PMMA_{50}$−PAA_{320}.

Table 1. Molecular Characteristics of the Synthesized Macromolecules

	M_w/M_n[a]	wt %[b]	M_w
$P2VP_{260}$	1.11	P2VP 83.9%	30000[c]
$P2VP_{260}$−$PMMA_{50}$	1.12	PMMA 15.1% P2VP 36.54%	35500[d]
$P2VP_{260}$−$PMMA_{50}$−$PtBA_{320}$	1.12	PMMA 6.9% PtBA 56.56% P2VP 49.6%	80500[d]
$P2VP_{260}$−$PMMA_{50}$−PAA_{320}		PMMA 9.1% PAA 41.3%	60500[d]

[a] Determined by means of SEC using PS standards. [b] Determined by means of ^{1}H NMR spectroscopy. [c] Determined by means of static light scattering in THF. [d] Calculated from M_w of the P2VP precursor and the composition.

Size Exclusion Chromatography. SEC of the P2VP and P2VP−PMMA and P2VP−PMMA−PtBA precursors was carried out using a set of three μ-Styragel columns of 103, 104, and 105 Å porosity and a differential refractometer as detector (model ERC-7515, ERC Inc.). The mobile phase was a 2% triethylamine solution in tetrahydrofuran and the flow rate 1 mL min^{-1}, assured by a Marathon II HPLC Pump coupled with a Pressure module (Rigas Labs). The calibration curve was obtained by PS standards.

Static Light Scattering. All the light-scattering experiments were carried out using a thermally regulated ((0.1 °C) spectrogoniometer, model SEM RD (Sematech France), equipped with a He−Ne laser (633 nm). The refractive index increments dn/dc required for the interpretation of the static light scattering measurements were determined using a Chromatic KMX-16 differential refractometer operating at 633 nm.

Dynamic Light Scattering. Dynamic light scattering technique was employed to characterize the hydrodynamic size of the micelles. The electric-field time correlation functions $g_1(\mathbf{q},t)$ were measured at various scattering angles and temperatures spanning a time scale from 10^{-7} to 10^3 s. The light source was an argon ion laser (Spectra Physics 2020) operating in single mode at 488 nm with a stabilized power of about 50 mW. The polarization conditions of the incident and scattered radiation were controlled by utilizing a set of a Glan and Glan-Thomson polarizers (Halle, Germany, and Berlin) with an extinction coefficient better than 10^{-7}. The scattered light was analyzed with a full multiple taut digital correlator (ALV-5000/E) with 280 channels. The time autocorrelation functions of the scattering intensity $g_2(\mathbf{q},t)$ were recorded with an ALV-5000/E fast multi-τ correlator in the real time scale from 10^{-7} to 10^3 s. The electric-field time correlation function $g_1(\mathbf{q},t)$ is related to the autocorrelation functions $g_2(\mathbf{q},t)$ by the Siegert relation

$$g_1(\mathbf{q},t) = [(g_2(\mathbf{q},t) - 1)/f^*]^{1/2} \quad (1)$$

where f^* is an instrument factor relating to the coherence area. The electric-field time correlation function $g_1(\mathbf{q},t)$ is the weighted sum of independent contributions coming from individual microdomains

$$g_1(\mathbf{q},t) = \int w(\mathbf{q},\tau) e^{(-t/\tau)}\, d\tau \quad (2)$$

where $w(\mathbf{q},\tau)$ is the distribution function of decay time τ, obtained by the inverse Laplace transformation (ILT) of the correlation function $g_1(\mathbf{q},t)$ using the CONTIN algorithm.

Diffusion coefficients were determined by eq 3

$$D = \langle\tau\rangle\mathbf{q}^2 \quad (3)$$

$\langle\tau\rangle$ being the average decay time.

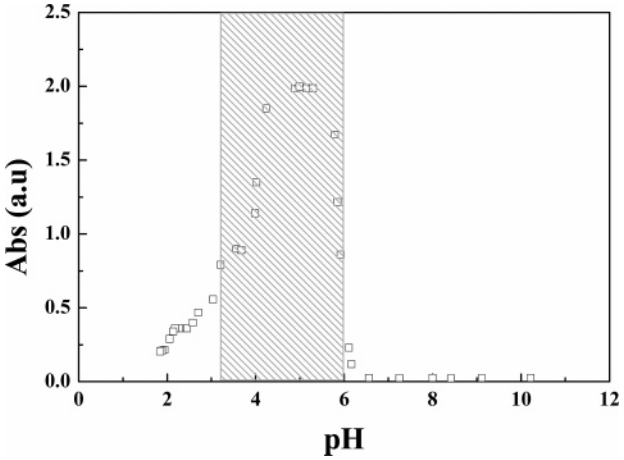

Figure 1. Variation of the optical density as a function of pH, for a 0.2 wt % aqueous solution of $P2VP_{260}-PMMA_{50}-PAA_{320}$.

Sample Preparation. The samples for the light scattering experiments were prepared by heating a stock solution at 80 °C for 12 h and allowed to equilibrate at room temperature overnight. Then the stock solution was diluted with pure water (Millipore) regulated at the desired pH to lower concentrations, and the samples were allowed to equilibrate for several hours. The pH of the solutions were corrected if needed before used.

Potentiometric Titration. Potentiometric titration was performed using a digital pH-meter 751 GPD Titrino (Metrohm), at 25 °C.

^{1}H NMR. ^{1}H NMR spectra were measured on a Bruker AC-200 spectrometer, at room temperature, in $CDCl_3$ or deuterated methanol.

Turbidity. Turbidity measurements were carried out using a U-2001 Hitachi spectrophotometer, operating at 490 nm and 25 °C.

Atomic Force Microscopy. Multimode AFM instrument (Digital Instruments, Santa Barbara) was operated in the tapping mode. Silicon tips with radius of 10−20 nm, spring constant of 30 N/m and resonance frequency of 250−300 kHz were used after calibration with gold nanoparticles (of diameter 5 nm) to evaluate the tip radius. The structure dimensions obtained from AFM images were corrected (decreased) by the tip radius.

Results and Discussion

The phase behavior of the $P2VP_{260}-PMMA_{50}-PAA_{320}$ in aqueous solutions was first explored by turbidity measurements in salt-free solutions at different pH. Figure 1 shows the optical density for a 0.2 wt % polymer as a function of pH. The existence of four regions can be observed. For pH < 2 the solutions are clear implying well dissolution of the polymer. The solutions become bluish and the optical density increases for 2 < pH < 3.2. At higher pH the solutions turn milky and the polymer precipitates revealing a two-phase region (3.2 < pH < 5.8). Finally at pH > 5.8, the polymer is redissolved, forming again homogeneous solutions. We should note that the polymer is not soluble directly in alkaline media but only after solubilization in low pH and addition of base.

Further exploration of the pH-dependent solution behavior of the system was conducted by static light scattering. In Figure 2, the intensity of the light scattered at an angle of 90°, I_{90}, of a 0.5 wt % polymer solution is presented as a function of pH. In the low pH region the scattered intensity, I_{90}, rises significantly from pH 2 to pH 3.2 while in the high pH region it remains at elevated values and nearly independent of

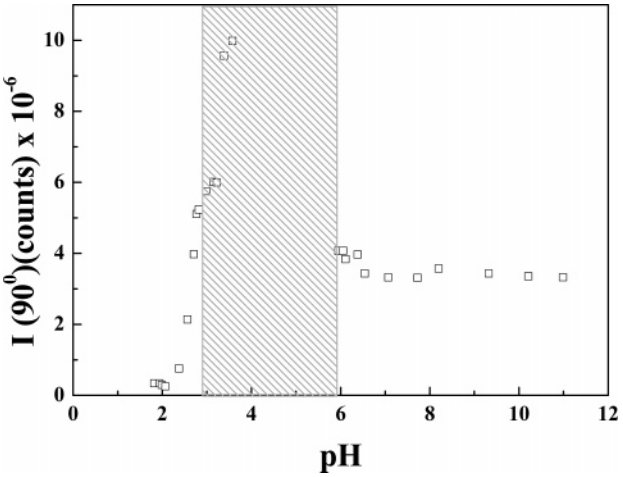

Figure 2. Variation of the light scattering intensity at 90° as a function of pH, for a 0.5 wt % aqueous solution of $P2VP_{260}-PMMA_{50}-PAA_{320}$, at 25 °C.

pH. In this pH region, the P2VP block is entirely deprotonated becoming hydrophobic while the PAA block is negatively charged. The hydrophilic−hydrophobic balance is shifted toward hydrophobic implying stronger association phenomena that result to strong light scattering. In the low pH region, P2VP is protonated and transformed to a water-soluble cationic weak polyelectrolyte. The hydrophilic−hydrophobic balance is then shifted toward hydrophilic and the light scattering intensity is weak close to pH 2. However, in the region 2 < pH < 3.2, both optical density and light scattering intensity increase, abruptly revealing intermolecular interactions between the different hydrophilic P2VP and PAA blocks.

The insoluble two-phase region, which is a usual behavior for diblock polyampholytes,[25,26] is located at pH between 3.2 and 5.8, the midpoint of which is at pH 4.5 and could be considered as the isoelectric point IEP (zero charge).[2,10] We observe that the IEP has been shifted to lower value with respect to that of $P2VP_{260}-PMMA_{50}-PAA_{320}$ (pH 5.5),[2] which should be attributed to the higher acid to base molar ratio (i.e., 1.22 against 0.42).[10]

Micelle Characterization in Solution by Light Scattering. The first information obtained from Figures 1 and 2 speaks for a stimuli responsive polymer, which self-assembles in different nanostructures depending on pH. The $P2VP_{260}-PMMA_{50}-PAA_{320}$ terpolymer under investigation was first solubilized in acidic media where P2VP and PAA are both water-soluble and only the middle PMMA block is hydrophobic. In such a case, heteroarm starlike micelles, with PMMA in the core and P2VP/PAA at the corona, are anticipated to be formed as have been shown for ABC terpolymers in selective solvents (bad solvent for the middle block; good solvent for the outer blocks).[13,23] However, the different kind of blocks in the corona are both sensitive to pH, since P2VP can be positively charged and PAA can be negatively charged, resulting to an amphoteric character for these micelles. Therefore, intra- and intermicellar electrostatic interactions (e.g., coulomb but also hydrogen bonding) and accordingly micelle transformation are expected to occur upon switching pH.

To determine the characteristics of the micelles in each pH region, static and dynamic light scattering experiments were carried out in aqueous solutions at pH 2, 3, and 10. In Figure 3, the concentration depen-

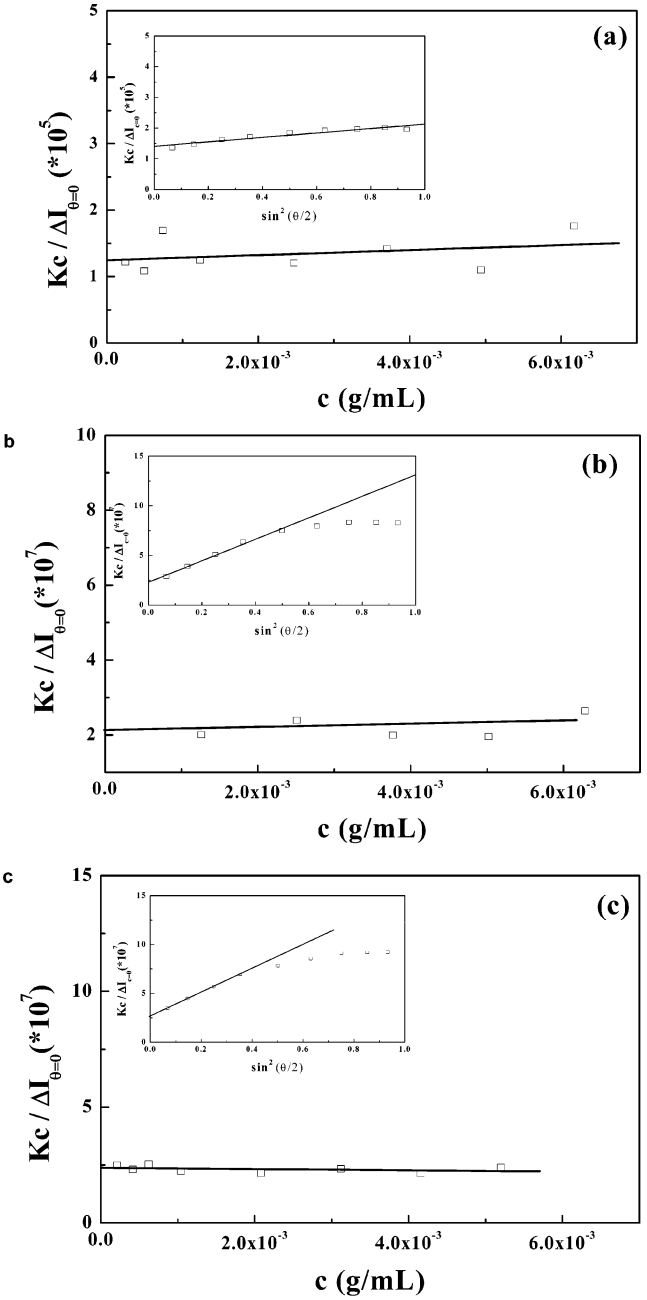

Figure 3. Concentration dependence of the inverse scattering intensity extrapolated to zero angle, $(Kc/\Delta I)_{\theta=0}$ of $P2VP_{260}-PMMA_{50}-PAA_{320}$ in water, at 25 °C and different pH values. In the inset, $(Kc/\Delta I)_{c=0}$ is plotted vs the scattering angle θ. Key: (a) pH = 2; (b) pH = 3; (c) pH = 10

dence of the inverse scattering intensity extrapolated to zero angle, $(Kc/\Delta I)_{\theta=0}$ where K is the optical constant and ΔI the scattering intensity difference between the solution and the solvent of $P2VP_{260}-PMMA_{50}-PAA_{320}$ is shown. From the extrapolated value at zero concentration, the apparent molecular weight of the micelles and therefore the aggregation number ($N_{agg} = M_{w,micelle}/M_{w,unimer}$) can be estimated. The apparent radius of gyration R_g of the formed micelles was calculated by the slope of the $(Kc/\Delta I)_{c=0}$ vs the scattering angle θ plots shown in the insets of Figure 3. At pH 3 and 10, a curvature in the angular dependence of $Kc/\Delta I$ was observed, and in such a case, slopes were obtained at low angles. The curvature is likely due to the size polydispersity of the micelles, and the determined radius corresponds mainly to the bigger micelles.

At pH 2, polymolecular micelles are formed with aggregation number $N_{agg} = 13$, and radius of gyration $R_g = 49$ nm. In this pH, P2VP is negatively charged, adopting a more or less stretched conformation,[27] while PAA is a weak acid with a coil conformation. Therefore, micellization is mainly due to the association of the hydrophobic PMMA moieties. Because PMMA is a glassy polymer, kinetically frozen micelles are expected to be formed.[27]

As pH rises from 2 to 3.2, intermolecular electrostatic interactions between the amphoteric polyelectrolyte blocks augments leading to an increase of the apparent aggregation number. At pH 3, $N_{agg} = 85$ and $R_g = 168$ nm, which is much higher than the contour length of the P2VP charged blocks (72 nm) implying nonmicellar aggregates. At even higher pH values more extending electrostatic interactions and the progressively transformation of P2VP to hydrophobic (insoluble at pH > 5) results in polymer precipitation.

At pHs higher than 6, the degree of ionization of the PAA blocks is adequate to solubilize again the polymer. At pH 10, the aggregation number is estimated to be $N_{agg} = 70$, and the radius of gyration is $R_g = 37$ nm. In this pH region, micellization is due to the association of PMMA and P2VP blocks.

More information about the hydrodynamic size and the size distribution of the formed micelles can be taken by dynamic light scattering measurements. Characteristic autocorrelation functions are presented in Figure 4. In the inset, the distribution of the relaxation times has been obtained by CONTIN analysis. Monomodal distributions can be observed showing a rather low size distribution of the micelles. In Figure 5, plots of diffusion coefficient as a function of concentration at pH 2 and 10 are depicted. Linear concentration dependence of D with negative slopes can be observed. It is known that

$$D = D_o(1 + K_D C + ...) \tag{4}$$

where D_o is the diffusion coefficient at infinite dilution and K_D is the concentration coefficient containing a thermodynamic and a hydrodynamic (frictional) component

$$K_D = 2A_2M_w - K_f - \nu \tag{5}$$

where A_2 is the second virial coefficient, M_w is the weight-average molecular weight of the diffusing species, K_f is the frictional coefficient, and ν is the partial specific volume of the polymer in the solvent. Since A_2 values are close to zero as obtained by static light scattering (see Figure 3), the hydrodynamic negative terms of eq 2 predominates, which gives the negative slopes. D_0 was used to determine the hydrodynamic radius R_H of the micelles according to the Stokes–Einstein equation

$$R_H = \frac{k_B T}{6\pi\eta D} \tag{6}$$

where k_B is the Boltzmann constant, T the absolute temperature, and η the solvent viscosity. The micelle characteristics determined by light scattering are summarized in Table 2.

As can be observed in Table 2, R_H decreases from pH 2 to 10 although the aggregation number increases. The size of the micelles is determined mainly from the

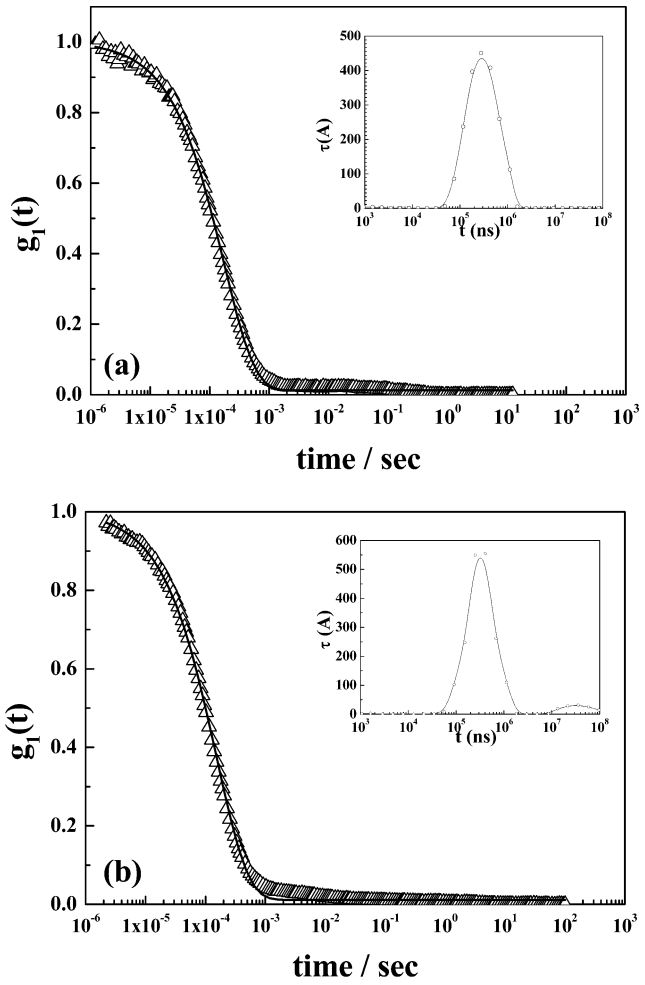

Figure 4. Time relaxation and correlation function for a 0.2 wt % solution of $P2VP_{260}-PMMA_{50}-PAA_{320}$, at 25 °C at pH = 2 (a) and pH = 10 (b).

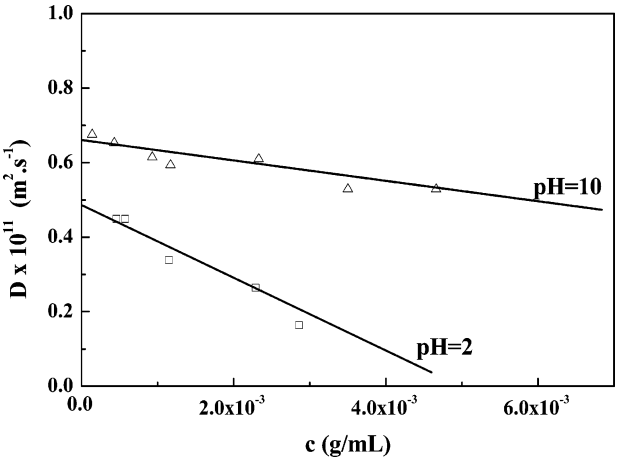

Figure 5. Variation of the diffusion coefficient as a function of concentration, at pH = 2 (□) and pH = 10 (Δ), at 25 °C.

conformation of the swollen chains in the corona (i.e., P2VP and PANa for the micelles at pH 2 and 10, respectively). Although the PAA length is longer than that of P2VP, the hydrodynamic radius of the micelles is smaller at pH 10. This could be attributed to the different degree of stretching of the corona chains. At pH 2, P2VP is protonated and adopts a stretched conformation. PAA is fully neutralized at pH 8 where the most extended conformation is expected. At pH 10, the ionic strength is elevated, and the screening effect

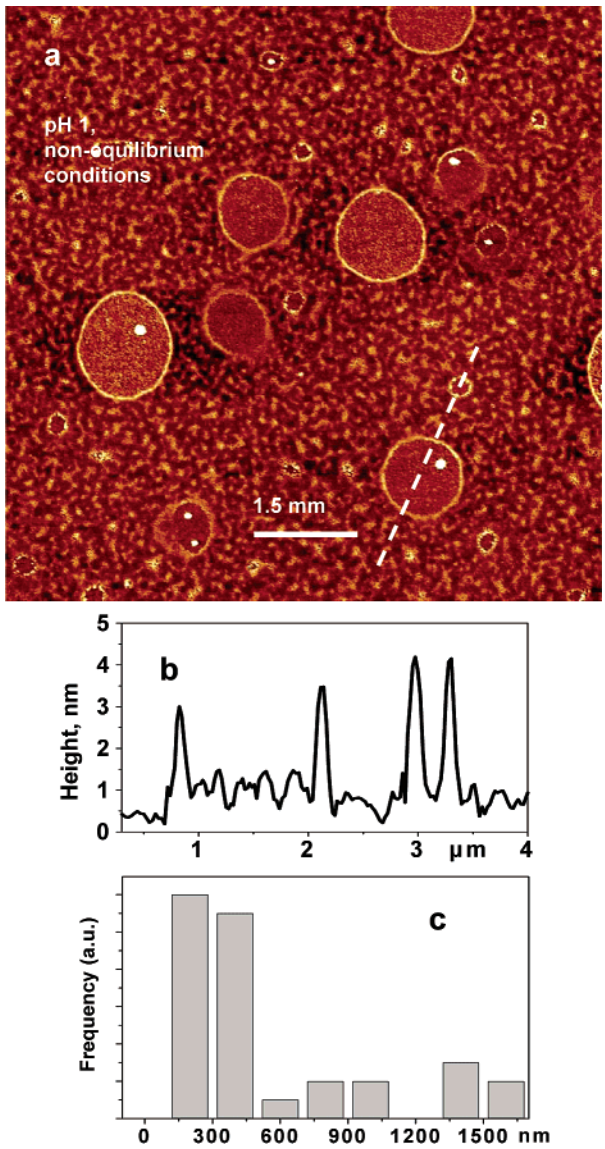

Figure 6. Representative AFM image (a), cross-section (b), and diameter distribution (c) of $P2VP_{260}-PMMA_{50}-PAA_{320}$ structures deposited from acid solutions (1 g/L, pH 1) in 1 h after the dissolution (sonication during 5 min).

Table 2. Micellar Characteristics in Different pH Values

	pH = 2	pH = 3	pH = 10
$M_{w(agg)}$	806 000	5141000	4212000
N_{agg}	13	85	70
R_g (nm)	49	168	37
R_H (nm)	44	nonmicellar aggregates	29
R_g/R_H	1.11		1.27

imposes lowering of the degree of stretching that is reflected in the smaller R_H.

Micelle Morphology on the Surface by AFM. To get deeper insight into the morphology and structure of the $P2VP_{260}-PMMA_{50}-PAA_{320}$ aggregates formed at different pH, an extensive AFM study was performed. To prepare the sample we set a drop of the solution onto the surface of freshly cleaved mica and afterward removed the rest of the drop with weak centrifugal forces. Previously we have shown that the so-deposited structures of polar polymer chains (for instance, protonated P2VP) appear to be trapped in a solution conformation due to strong attraction to the surface of polar mica. On the other hand, nonpolar polymers undergo relatively fast relaxation on the surface upon exposure

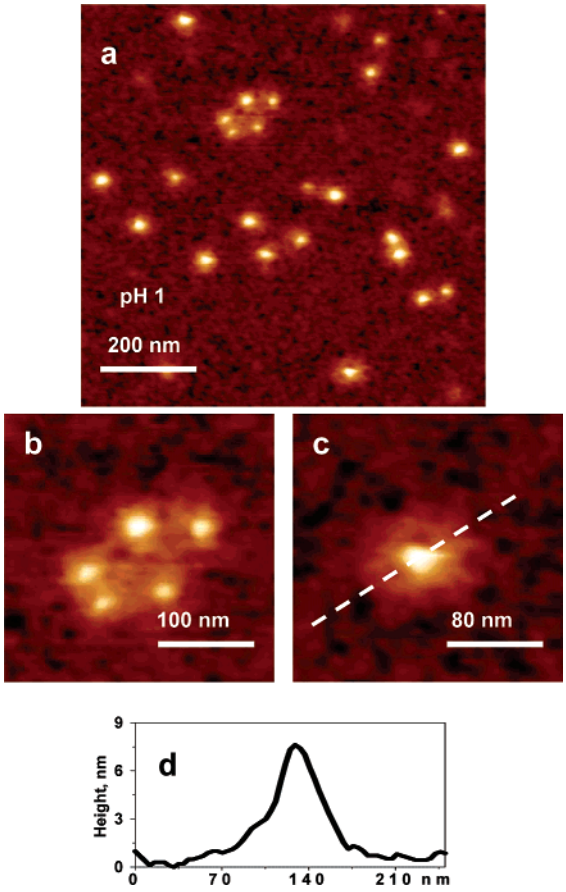

Figure 7. AFM images (a–c) and cross-section (d) of $P2VP_{260}$–$PMMA_{50}$–PAA_{320} structures deposited from acid solutions (1 g/L, pH 1) in 10 h after the polymer dissolution.

in good solvents, because of weak interactions between the polymer and mica. Because of the high content of polar blocks in the $P2VP_{260}$–$PMMA_{50}$–PAA_{320} macromolecular chain, one can expect rather good correspondence between morphologies of aggregates in solutions and morphologies of aggregates immobilized onto polar substrates.[28]

Figures 6–8 show the evolution in time of aggregates formed at pH 1. The solution (1 mg/mL) was prepared upon brief sonication (5 min) at elevated temperature (60 °C) in acidic water (pH 1, HCl) and then allowed to equilibrate at room temperature. Figure 6–8 show AFM images of $P2VP_{260}$–$PMMA_{50}$–PAA_{320} adsorbed after 1, 10, and 240 h after the dissolution of the polymer, respectively. As seen in Figure 6, deposition of the freshly prepared polymer solution results in circular structures, which correspond to vesicles, projected onto the surface upon the adsorption and evaporation of the solvent. Although the outside diameter of the vesicles varies in a broad range between 100 nm and 1.5 μm, they have rather uniform wall thickness of about 70–90 nm. Similar structures formed upon dissolution of block copolymers with amphoteric blocks have also been described recently.[19,25,29] In the case of a quite similar system (PAA_{28}–PS_{890}–$P4VP_{40}$), which however differs significantly in monomer composition, polymeric vesicles are also formed at pH 1.[19] The stabilization of these aggregates is due to the fact that the soluble corona-forming blocks are very short relative to the insoluble core-forming block. In the opposite case, when the stabilized blocks are long enough, block copolymers tend to form starlike micelles. Therefore, it was somewhat

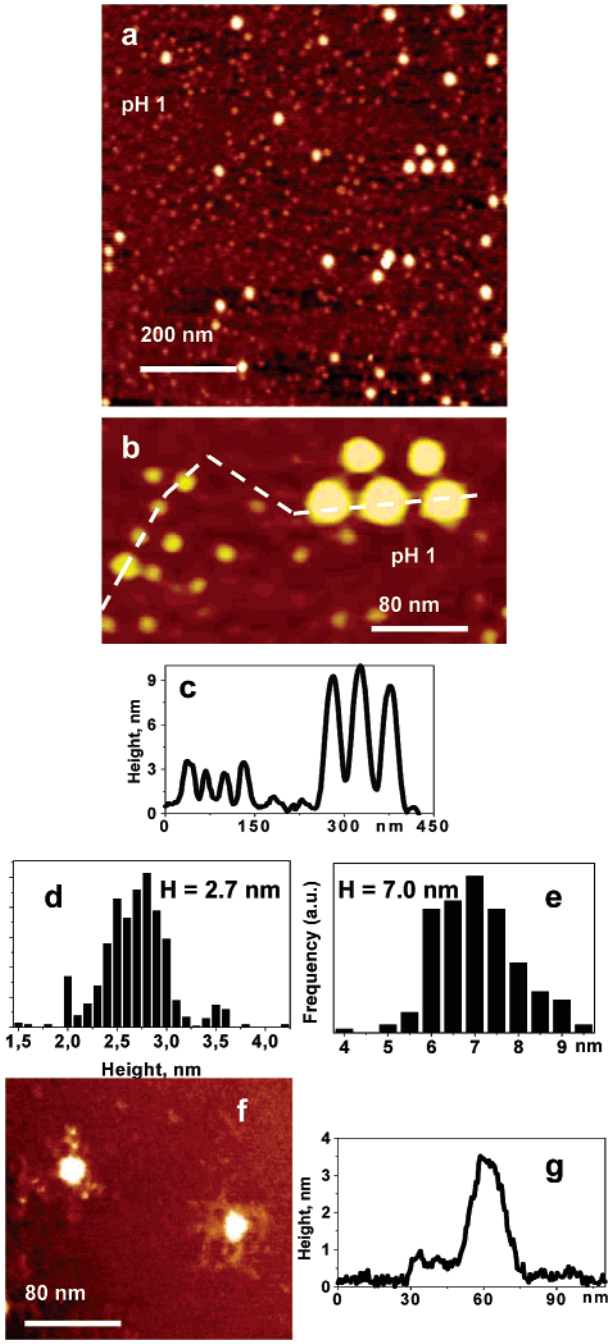

Figure 8. AFM images (a, b), cross-section (c), and height distributions of $P2VP_{260}$–$PMMA_{50}$–PAA_{320} unimers (d) and micelles (e) deposited from acid solutions (1 g/L, pH 1) in 10 days after the polymer dissolution. The image of $P2VP_6$–PS_6 unimers (f) and the cross-section (g) having the same length of P2VP blocks as in P–M–A, adsorbed at pH 1 are given for comparison.

surprising to observe the formation of vesicles in our case, since the core-forming PMMA block is very short. A considerable amount of the material, however, exists in the nonaggregated state and localizes outside of the vesicles. Thus, $P2VP_{260}$–$PMMA_{50}$–PAA_{320} displays a rather weak capability to aggregate at pH 1, where the P2VP block is significantly charged. Indeed the vesicles were found to be unstable and were transformed to heteroarm starlike micelles, of 5–6 nm in height and up to 60–90 nm in diameter, after 10 h of equilibration (Figure 7).

Figure 8 presents nanoparticles, deposited from the solution, which were allowed to equilibrate at pH 1

Scheme 1

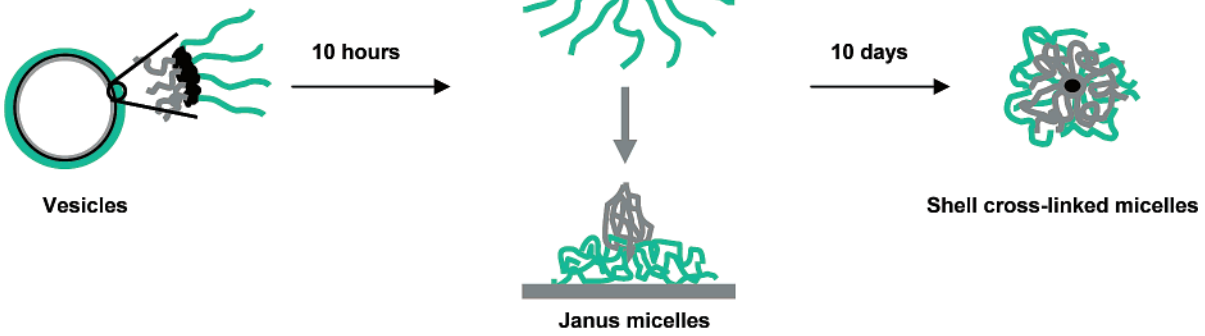

during more than 10 days. The smaller particles have a height of about 2.7 nm and a diameter of approximately 12 nm. The mean volume of the smaller particles estimated on the base of the AFM data is equal to 101 nm^3, which is very close to the theoretical volume of the $P2VP_{260}-PMMA_{50}-PAA_{320}$ unimer. The particles of the second type in the image (Figure 8) have a mean height of about 7 nm and a mean diameter of 34 nm.

It was previously shown that P2VP-comprising block copolymers (such as heteroarm stars PS_7P2VP_7) form starlike unimolecular and/or polymolecular micelles with low aggregation number in acidic solutions, and those micelles can be nicely resolved upon the AFM imaging onto atomically flat mica.[30a] In that case, the hydrophobic blocks collapse and form the core of the micelles, whereas protonated P2VP arms appear in the extended conformation and constitute the shell. The protonated P2VP chains interact strongly with the polar mica; thus their conformation is retained upon evaporation of the solvent and even during a long-time exposure in bad solvents. As an example, parts f and g of Figure 8 show an AFM image and the cross section of the PS_6P2VP_6 unimers adsorbed from acid water (pH 1). P2VP arms in PS_6P2VP_6 have the same length as in $P2VP_{260}-PMMA_{50}-PAA_{320}$, and the diameter of the shell is about of 60−70 nm. In this regards, the starlike micelles with a core−shell structure shown in Figure 7, formed from early stages of the equilibration, fit our expectation. In contrast, the equilibrium morphology of the $P2VP_{260}-PMMA_{50}-PAA_{320}$ micelles appears on AFM images as smooth spheres (or at least, the core−shell structure cannot be resolved by AFM, Figure 8). A plausible explanation of this shell-structure aging effect could be the following. In the early stage of micellization, Janus micelles (segregation of the different arms in the corona) may be formed. The P2VP positively charged arms are adsorbed on the negatively charged substrate, and since they adopt a stretched conformation, they can be nicely resolved from the PAA chains, which adopt a coillike conformation and are not adsorbed on the surface (Scheme 1). Although, a significant fraction of P2VP units is protonated at pH 1, certainly some pyridine units still retain in the base state and could develop hydrogen bonding with the nondissociated PAA units[16] with time. Thus, the arm segregation progressively is destroyed (no Janus configuration), and the shell appears to be constituted by a mixture of P2VP and PAA chains stabilized by hydrogen bonding. The time dependent phenomena of the structural transformation of the micelles at pH 1 are schematically shown in Scheme 1.

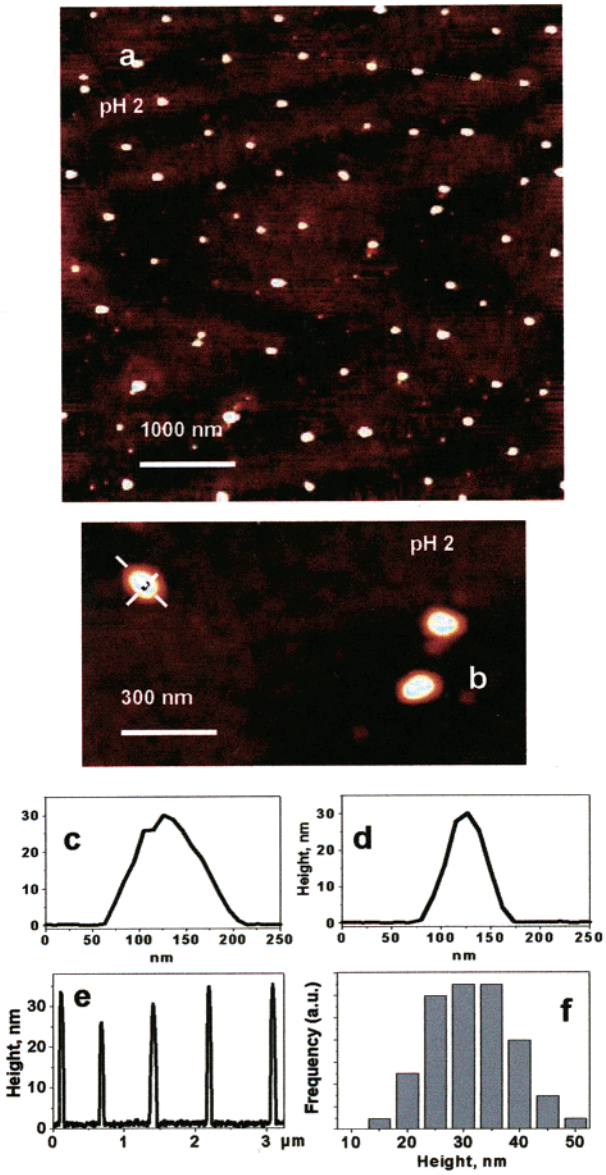

Figure 9. Representative AFM images (a, b), cross sections (c−e), and heights distribution of $P2VP_{260}-PMMA_{50}-PAA_{320}$ structures deposited from the solution at pH 2. Cross-sections c and d correspond to the lines in image b; cross-section e corresponds to the line in image a.

At higher pH $P2VP_{260}-PMMA_{50}-PAA_{320}$ undergoes further association into larger aggregates. Figure 9 shows nearly monodisperse slightly ellipsoid micelles

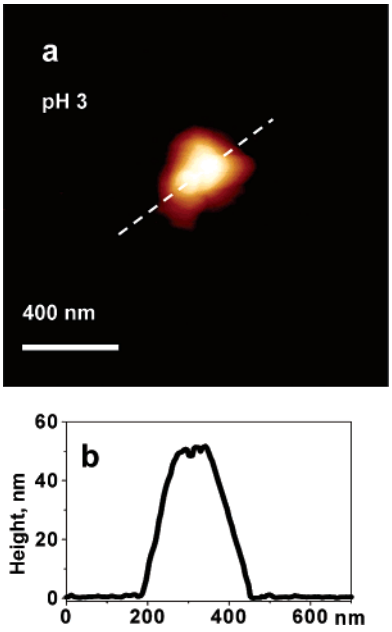

Figure 10. AFM image (a) and cross-section (b) of $P2VP_{260}-PMMA_{50}-PAA_{320}$ structures deposited from acidic solution (pH 3).

formed at pH 2. They are of 31.6 nm in the height and of 60 nm in the short semiaxes length and 100 nm in the long semiaxes length. No resolved shell is observed around the particles and all the material is associated since no unimers are visible around the micelles. The elongated shape and the size of these micelles is in good agreement with the value of the ratio $R_g/R_H = 1.11$ (0,75 for hard spheres) and the mean diameter (88 nm of a equivalent sphere) determined by light scattering.

Only nonuniform big objects with more than 200 nm in diameter were found at pH 3 (Figure 10) again in very good agreement with the light scattering results. At this pH, intermicellar coulomb electrostatic interactions between the different corona chains predominate, leading to big irregular aggregates. The same kind of interaction has led to the formation of a physical network for the $PAA_{134}-P2VP_{628}-PAA_{134}$ copolymer as we have observed recently.[2,3]

All these results fit to our hypothesis of the formation of micelles with interactive chains in the corona. The drastic increase of the aggregation number upon switching pH from pH 1 to pH 3 could not be attributed to the changing of the solvent quality. Indeed, it is well-known that P2VP is readily soluble and adopts an extended conformation at any pH, lower than pH 4. Previously we showed that aggregation number of $P2VP_7-PS_7$ star-shaped block copolymers at fixed polymer concentration was almost independent of pH in the range from pH 1 to 4, and even partial protonation of P2VP chains is enough to stabilize micelles. On the other hand, the presence of nondissociated PAA and nonprotonated pyridine units at the same time leads to the formation of complexes through hydrogen bonding and/or oppositely charge interactions. Although the complexation of homopolyelectrolyte homopolymers usually leads to the formation of insoluble aggregates, which precipitate in aqueous solution, the $P2VP_{260}-PMMA_{50}-PAA_{320}$ structures formed in acid solution are remarkable stable due to excess of protonated P2VP and free PAA units. To the best of our knowledge, we described the first example of stable shell cross-linked micelles formed simply by dissolution of *single* ABC terpolymers, composed of A and C water-soluble blocks.

In the basic conditions when acrylic acid units are ionized, the formation of negatively charged particles is expected. The mica surface, however, is also negatively charged at this conditions that would suppress adsorption. Indeed, we found no adsorption at this pH range, and therefore, $P2VP_{288}-PMMA_{55}-PAA_{351}$ was deposited by drying a droplet and gently rinsing the substrate with water.

Spherical micelles were expected to form with a double layer (P2VP/PMMA) centrosymmetric core surrounded by a PAA charged corona, in the same way as ABC terpolymers, with A and B hydrophobic blocks,[17] and/or amphiphilic heteroarm star copolymers form polymolecular micelles.[30] Surprisingly instead of that, loosely packed aggregates of small nearly spherical micelles together with big particles can be seen in Figure 11. It should be noted here that the polymer is not soluble directly under basic conditions showing that equilibrium is difficult to attain. The structure shown

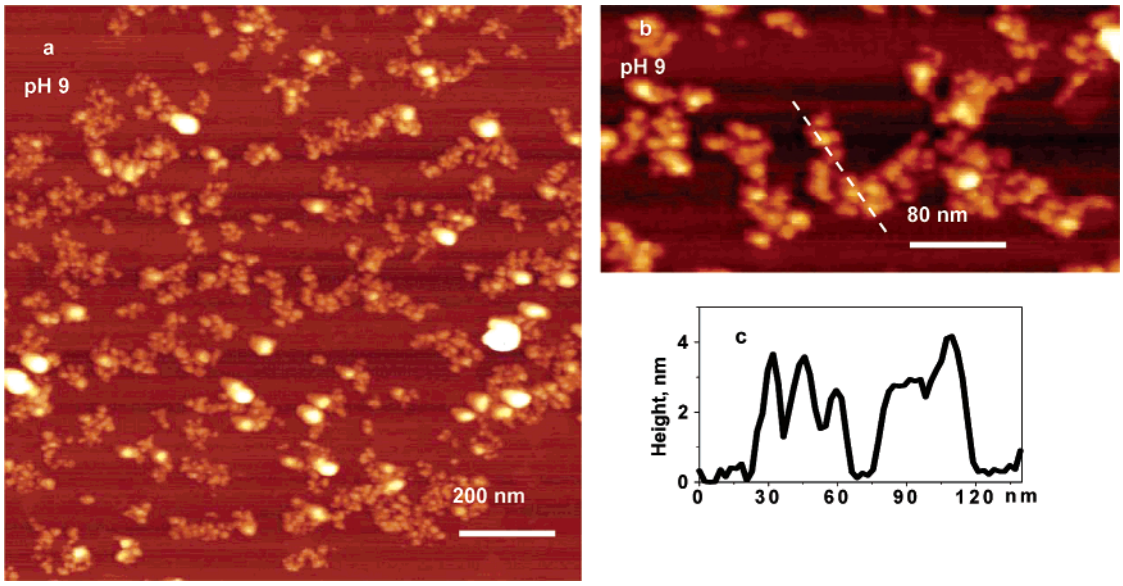

Figure 11. AFM images (a, b) and cross-section (c) of $P2VP_{260}-PMMA_{50}-PAA_{320}$ structures deposited from basic solution (pH 9). A drop of the solution was allowed to evaporate onto the mica surface and then was rinsed with water.

in Figure 11 resulted from the solution of pH 1 by adding some drops of concentrated NaOH. This kind of morphology has also been observed for the so-called Janus micelles very recently. [31] In fact these Janus micelles are heteroarm star copolymers with equal PS and PMA arms emanated from a cross-linked PB core. Since they have been prepared from a microphase separated structure in the bulk state they exhibit arm segregation at will, i.e., PS and PMAA hemispheres, which should persist in solution of a selective solvent. There are obvious similarities between these amphiphilic systems. In our case, at low pH heteroarm starlike micelles are formed constituted of a PMMA glassy hydrophobic core bearing P2VP and PAA arms in the corona. By switching pH and passing to the alkaline region, P2VP is transformed to a glassy hydrophobic polymer similar to PS while the PAA arms constitute the soluble part similar to PMA. Therefore, it is reasonable to assume that real ABC Janus micelles (without being cross-linked but probably frozen in the middle block) are formed, due to segregation of the corona arms that is driven by the strong selectivity of the solvent and the incompatibility between P2VP and PANa. Since P2VP is hydrophobic at basic conditions further aggregation of the Janus micelles occur leading to the formation of micellar clusters (Figure 11).

This unexpected morphology seems to be out-of-equilibrium. The size of the nanoparticles that are incorporated in the clusters are of comparable size with those they originated from (pH 1). This implies that micelles with frozen cores have been formed at pH 1. By switching the pH to 11, the PAA arms are extended due to the repulsive interactions, while the P2VP arms are collapsed toward to the PMMA cores in a manner similar to what PS arms do in unimolecular micelles formed by PS_7P2VP_7 in aqueous acidic media.[30a] Nevertheless, due to the unfavored hydrophobic−hydrophilic ratio they further tend to aggregate, not into the thermodynamically more favored spherical micelles (since they are frozen) but into long loose associates. An alternative interpretation of the negatively charged micelle association into clusters may account for intermicellar electrostatic attractive interactions due to counterion cloud fluctuations as suggested for spherical polyelectrolyte microgels.[32]

This aggregation occurs in some extend in solution since we found a higher aggregation number by light scattering. However, evaporation of the solvent on the surface as well as surface interactions may be involved in the aggregation process, and this makes difficult a direct correlation between light scattering and AFM results in this case.

Conclusions

A water-soluble ABC block terpolymer with a hydrophobic middle block and amphoteric hydrophilic A and C blocks was synthesized by anionic polymerization and explored in aqueous solutions by light scattering and atomic force microscopy. An interesting phase behavior and self-assembling of this ABC terpolymer with interactive A and C blocks was observed by switching the pH of the solution.

Several pH regions can be distinguished. In the acidic pH region and at low pH (1−2) heteroarm starlike micelles are formed with interactive P2VP and PAA chains at the corona. Intramicellar interactions due to hydrogen bonding, induce transformation of the corona structure from a two-compartment shell (Janus micelles with segregated arms) to a weak cross-linked shell (mixed arms). As pH increases from 2 to 3, electrostatic intermicellar attractive interactions rise, leading to the formation of nonregular aggregates. An insoluble two-phase region around the isoelectric point of the amphoteric chains was observed between pH 3.2 and 5.8. Finally, by switching pH in alkaline media, an unexpected and probably out of equilibrium morphology, of aggregated heteroarm starlike amphiphilic micelles, was observed on mica substrate.

Acknowledgment. The authors are grateful for the financial support provided by the IKY (Greece) and DFG (Germany). This work was performed in the framework of the cooperation program between Greece and Germany IKYDA 2002. A.K. is grateful for the financial support provided by the DFG/CNRS German−French bilateral program (Project STA 324/13-1). We would like to thank Prof. Minko for helpful discussions.

References and Notes

(1) (a) Kudaibergenov, S. E. *Adv. Polym. Sci.* **1999**, *144*, 115. (b) Lowe, A. B.; McCornick, C. L. *Chem. Rev.* **2000**, *102*, 4177.
(2) Sfika, V.; Tsitsilianis, C. *Macromolecules* **2003**, *36*, 4983.
(3) Bossard, F.; Sfika, V.;Tsitsilianis, C. *Macromolecules* **2004**, *37*, 3899.
(4) (a) Leibler, L.; Fredrickson, G. H. *Chem. Br.* **1995**, 42−45. (b) Bates, F. S.; Fredrickson, G. H. *Phys. Today* **1999**, *52*, 32.
(5) Kudose, I.; Kotaka, T. *Macromolecules* **1984**, *17*, 2325.
(6) Mogi, Y. Mori, K. Matsushita, Y.; Noda, I. *Macromolecules* **1992**, *25*, 5412.
(7) Auschra, C.; Stadler, R. *Macromolecules* **1993**, *26*, 2171.
(8) Gido, S. P.; Schwark, D. W.; Thomas, E. L.; Goncalves, M. C. *Macromolecules* **1993**, *26*, 2636. Lohse, D. J.; Hadjichristidis, N. *Curr. Opin. Colloid Interface Sci.* **1997**, *2*, 171.
(9) Lazzani, M.; López-Quintela, M. *Adv. Mater.* **2003**, *15*, 1583.
(10) Patrickios, C. S.; Hertler, W. R.; Abbott, N. L.; Hatton, T. A. *Macromolecules* **1994**, *27*, 930.
(11) Chen, W.-Y.; Alexandridis, P.; Su, C.-K.; Patrickios,; C. S.; Hertler, C. S.; Hatton, T. A. *Macromolecules* **1995**, *28*, 8604.
(12) Patrickios, C. S.; Forder, C.; Armes, S. P.; Billingham, N. C. *J. Polym. Sci., Part A: Polym. Chem.* **1997**, *35*, 1181.
(13) Patrickios, C. S.; Lowe, A. B.; Armes, S. P.; Billingham, N. C. *J. Polym. Sci., Part A: Polym. Chem.* **1998**, *36*, 617.
(14) Gohy, J.-F.; Willet, N.; Varshney, S.; Zhang, J.-X.; Jérôme, R. *Angew. Chem.* **2001**, *113*, 3314.
(15) Triftaridou, A. I.; Vamvakaki, M.; Patrickios, C. S. *Polymer* **2002,** *43,* 2921−2926.
(16) Giebeler, E.; Stadler, R. *Macromol. Chem. Phys.* **1997**, *198*, 3815.
(17) Kriz, J.; Masar, B.; Plestil, J.; Tuzar, Z.; Pospisil, H.; Doskocilova, D. *Macromolecules* **1998**, *31*, 41.
(18) Yu, G.; Eisenberg, A. *Macromolecules* **1998**, *31*, 5546.
(19) Liu, F.; Eisenberg, A. *J. Am. Chem. Soc.* **2003**, *125*, 15059.
(20) Liu, S.; Weaver, J. V. M.; Tang, Y.; Billingham, N. C. Armes, S. P.; Tribe, K. *Macromolecules* **2002**, *35*, 6121.
(21) Saito, R.; Fujita, A.; Ichimura, A.; Ishizu, K. *J. Polym. Sci., Polym. Chem. Ed.* **2000**, *38*, 2091.
(22) Erhardt, R.; Böker, A.; Zettl, H.; Kaya, H.; Pyckhout-Hintzen, W.; Krausch, G.; Abetz, V.; Müller, A. H. E. *Macromolecules* **2001**, *34*, 1069−1075.
(23) Tsitsilianis, C.; Sfika, V. *Macromol. Rapid Commun.* **2001**, *22*, 647.
(24) Tsitsilianis, C.; Chaumont, P.; Rempp, P. *Makromol. Chem.* **1990**, *191*, 2319.
(25) Gohy, J.-F.; Creutz, S.; Garcia, M.; Mahltig, B.; Stamm, M.; Jérôme, R. *Macromolecules* **2000**, *33*, 6378.
(26) Liu, S.; Armes, S. P. *Angew. Chem.* **2002**, *114*, 1471.
(27) Rager, T.; Meyer, W. H.; Wegner, G.; Winnik, M. A. *Macromolecules* **1997**, *30*, 4911.
(28) (a) Minko, S.; Kiriy, A.; Gorodyska, G.; Stamm, M. *J. Am. Chem. Soc.*; **2002**, *124*, 3218. (b) Gorodyska, A.; Kiriy, A.; Minko, S.; Tsitsilianis**,** C.; Stamm, M. *Nano Lett.* **2003**, *3,* 365−368.

(29) Bieringer, R.; Abetz, V.; Müller, A. H. E. *Eur. Phys. J.* **2001** *5*, 5.
(30) (a) Kiriy, A.; Gorodyska, G.; Minko, S.; Stamm, M.; Tsitsilianis, C. *Macromolecules* **2003**, *36*, 8704. (b) Voulgaris, D.; Tsitsilianis, C.; Esselink, F.; Hadziioannou, G. *Polymer* **1998**, *39*, 6429. (c) Voulgaris, D.; Tsitsilianis, C.; Grayer, V.; Esselink, F.; Hadziioannou,; G. Polymer **1999**, *40*, 5879. (d) Tsitsilianis, C.; Voulgaris, D.; Štěpánek, M.; Podhájecká, K.; Procházka, K.; Tuzar, Z.; Brown, W. *Langmuir* **2000**, *16,* 6868.
(31) Erhardt, R.; Zhang, M.; Boker, A. Zettl, H.; Abetz, C.; Frederic, P.; Krausch, G.; Abetz, V.; Müller, A. *J. Am. Chem. Soc.* **2003**, *125*, 3260.
(32) Grohn, F.; Antonietti, M. *Macromolecules* **2000**, *33*, 5938.

MA048621Q